Chinese Chemical Letters 33 (2022) 3087–3090

Contents lists available at ScienceDirect

Chinese Chemical Letters

journal homepage: www.elsevier.com/locate/cclet

Development of Mn-Si-MEL as a bi-functional adsorption-catalytic oxidation material for VOCs elimination

Qingjun Yu[a,b], Yongchao Feng[a], Jinghui Wei[a], Xiaolong Tang[a,b], Honghong Yi[a,b,*]

[a] School of Energy and Environmental Engineering, University of Science and Technology Beijing, Beijing 100083, China
[b] Beijing Key Laboratory of Recycling of Typical Industrial Pollutants, Beijing 100083, China

ARTICLE INFO

Article history:
Received 4 August 2021
Revised 2 September 2021
Accepted 22 September 2021
Available online 26 September 2021

Keywords:
Bifunctional
Adsorption
Catalytic combustion
VOCs
MEL
Mn-Si

ABSTRACT

Mn-Si-MEL zeolite was developed as a bi-functional adsorption-catalytic oxidation material for volatile organic compounds (VOCs) elimination due to its good hydrophobicity & good organophileproperty brought by the substitution of Mn for Al in zeolite and the superior catalytic oxidation property endowed by the existence of Mn species. Various Mn-Si-MEL samples were obtained by introducing Mn to MEL crystallization system *via* different ways. It was found the incorporated Mn ways have a significant effect on the behavior of Mn being involved in the crystallization of MEL and finally influenced the distribution of Mn in zeolite as well the physicochemical properties of product zeolite. The seeding method (Mn-S2(Seed)) is favorable for the good incorporation and uniform distribution of Mn in zeolite while both recrystallization method (Mn-S2(RC)) and direct synthesis method (Mn-S2(DH)) are favorable for obtaining more reducible Mn species and surface adsorbed oxygen species. The Mn amount incorporated into zeolite follows Mn-S2(RC) (1.96 wt%) > Mn-S2(Seed) (1.07 wt%) ≈ Mn-S2(DH) (0.97 wt%), the adsorption capacity of various samples follows Mn-S2(Seed) (83.3 μmol/g) ≈ Mn-S2(RC) (82.1 μmol/g) > Mn-S2(DH) (76.1 μmol/g), while the catalytic oxidation ability of three samples follows Mn-S2(RC) ≈ Mn-S2(DH) > Mn-S2(Seed). Furthermore, Mn-S2(RC) which exhibits both superior adsorption capacity and catalytic oxidation ability shows good hydrophobicity and superior recyclability, demonstrating its great potential to be applied in the VOCs elimination by an enrichment-degradation route.

As an important contributor to the numerous environmental problems like ground-level ozone, photochemical smog, PM2.5, *etc.*, volatile organic compounds (VOCs) emitted from stationary and mobile sources cause great attention from both the government and researchers. Among various existing technologies, catalytic combustion was viewed as an efficient and environmental friendliness route to convert hazardous VOCs to CO_2 completely [1,2]. Nevertheless, this method is not suitable for the purification of exhaust gas with low concentration of VOCs. Therefore, adsorption was commonly applied to combine with the combustion unit to realize the first enrichment of VOCs as well as to reduce the energy consumption during the subsequent combustion process [3-5]. During this process, the complete desorption of VOCs from the adsorbents seems to be key for ensuring the operation of this technique for regenerating the adsorbent and providing high-concentrated VOCs for the subsequent combustion unit. Due to the combination of various units, the adsorption-combustion technique seems to be a complicated and long process. In order to overcome these drawbacks described above, dual functional adsorbent-catalyst media was proposed to develop for integrating the function of adsorption and catalytic combustion so that the process and operation could be greatly simplified [6-8].

Zeolites have been regarded as superior adsorbents due to their large specific surface area, high adsorption capacity, superior thermal & hydrothermal stability, non-flammability as well as their tailored properties [9,10]. Additionally, after doping with metals, the zeolite-supported metal materials were also viewed as highly efficient catalysts for the combustion of VOCs [11-14]. In 2004, Baek, Kim and Ihm proposed to apply metal loaded on hydrophobic HY as a dual functional adsorbent/catalyst media for the control of low concentrated VOC streams and Ag/HY was selected to be the best candidate for the dual functional adsorption-catalytic oxidation system for methylethylketone and toluene abatement [6]. In recent reports, Ru/HZSM-5 was developed for being applied in the combined adsorption-combustion method for eliminating bulky aromatics (toluene *o*-xylene and 1,3,5-trimethylbenzene) with low concentration levels [8]. In a word, both good organophileproperty and superior catalytic oxidation property are prerequisite for being

* Corresponding author.
E-mail address: yhhtxl@163.com (H. Yi).

https://doi.org/10.1016/j.cclet.2021.09.072
1001-8417/

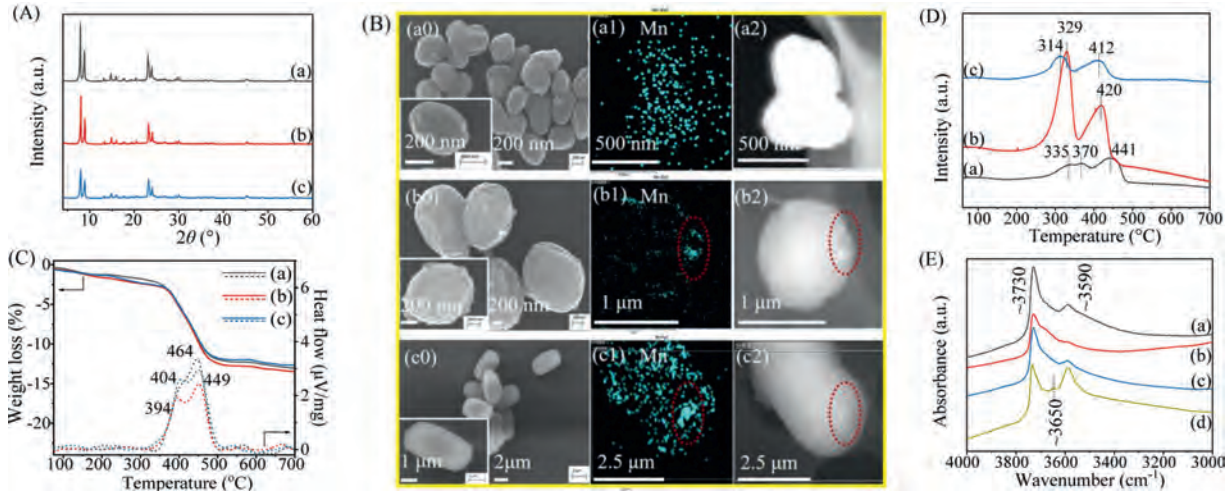

Fig. 1. (A) XRD patterns, (B) Scanning electron microscope (SEM) (a0-c0) & scanning transmission electron microscope (STEM)-mapping (a1-c2), (C) Thermogravimetric-differential thermal analysis (TG-DTA), (D) H_2-temperature programmed reduction (H_2-TPR) and (E) IR spectra of OH region of Mn-Si-MEL samples synthesized by different methods. (a) Mn-S2(Seed), (b) Mn-S2(RC), (c) Mn-S2(DH).

a dual functional adsorption-catalytic oxidation material. Moreover, good hydrophobicity is also necessary for this material to be applicable in moisture VOCs exhaust purification.

In our previous study, it was found that after substituting Al in zeolite for transition metal (Fe, Cu, Mn), the obtained metal-silicalite could behave as a dual functional adsorption-catalytic oxidation material applied in the non-methane hydrocarbon (NMHC) removal from cooking oil fumes (COFs) [15,16]. Among various metal-silicalite samples, Mn-silicalite displays both good adsorption capacity and higher catalytic oxidation performance for NMHC in COFs than other samples. Hence, in this work, various Mn-Si-MEL samples were developed and comprehensively investigated to be a superior bi-functional adsorption-catalytic oxidation candidate for possessing the properties of organophileproperty, catalytic oxidation property as well as hydrophobicity simultaneously. In detail, Mn-containing source was introduced into the synthesis system of MEL (an end member of the pentasil family, possessing intersecting straight channels with a pore size of 5.3 Å × 5.4 Å, tailored Si/Al ratio until ∞, Fig. S1 in Supporting information) instead of the conventional Al source. Different introduction ways were performed (see S2 Synthesis in Supporting information) and the corresponding types & distribution of Mn species in MEL as well as their effect on the obtained samples' adsorption-catalytic oxidation properties were investigated and analyzed. Fig. 1A shows the X-ray diffraction (XRD) patterns of Mn-Si-MEL samples obtained *via* seeding method (Mn-S2(Seed)), recrystallization method (Mn-S2(RC)) and direct synthesis method (Mn-S2(DH)), respectively. Typical characteristic diffraction peaks of MEL topology at 2θ of 7.92°, 8.78°, 23.14°, 23.98° and 45.2° are observed in all three samples, confirming the successful formation of MEL framework without being influenced by the introduction of Mn. Both the different morphologies (Figs. 1B (a0-c0)) of Mn-Si-MEL samples from the conventional Al-Si-MEL reported in our previous study [17-19] and the ICP results (Table 1) demonstrate that Mn has been well involved into zeolite crystallization process. The actual Mn content incorporated into zeolite follows the sequence of Mn-S2(RC) > Mn-S2(Seed) ≈ Mn-S2(DH) when the same amount of Mn source was added into three systems. The SEM images also reflect the crystal size of zeolite samples. An evident difference in crystal size was found among three samples, following the sequence of Mn-S2(Seed) < Mn-S2(RC) < Mn-S2(DH). Taking account of our previous study [18,20], it is well known that the presence of seeds is favorable for the quick formation of numerous nuclei and hence results in large amounts of small crystals. In contrast, in the system with no seed, if the Mn source was added to form the initial gel, it will participate in both nucleation and crystal growth process. The involution of Mn into zeolitic structure unit decelerates the formation rate of framework compared with the silicate system. As a sequence, fewer nuclei will be generated and subsequently grow into large crystals of Mn-S2(DH). Noting that the Mn-S2(RC) exhibits smaller crystal size than Mn-S2(DH) despite of being synthesized from the system absence of seed. This is related to the adding time of Mn into the system. Different from introducing Mn into the initial gel of Mn-S2(DH), for Mn-S2(RC), Mn was added into the system with well crystallized silicalite-2, whose nucleation is much faster in the silicate gel than that in the Mn-containing gel. The extraneous Mn introduced into the crystallized system causes the unbalance of species & the variation of crystallization environment, and therefore lead to the dissolution of silicalite-2 framework and the new formation of Mn-containing framework during recrystallization process. Hence, the crystal size of Mn-S2(RC) was well retained from silicalite-2 but the morphology varies from the single-like crystal of silicalite-2 (Fig. 4d in reference [17]) to the crystal-stacking morphology of Mn-S2(RC) due to the fact that the additional Mn participate in the recrystallization of zeolite.

Table 1
Textural properties & sorption capacity of various Mn-Si-MEL samples.

Sample		Mn-S2(Seed)	Mn-S2(RC)	Mn-S2(DH)
Mn (wt%)		1.07	1.96	0.97
Pore characterization	S_{BET} (m^2/g)	427.9	401.0	407.6
	S_{micro} (m^2/g)	311.7	252.5	280.3
	S_{ext} (m^2/g)	116.2	148.5	127.3
	V_{micro} (cm^3/g)	0.12	0.10	0.11
	V_{meso} (cm^3/g)	0.13	0.17	0.12
Relative atomic ratio (%)	Mn 2p/Mn^{4+}	30.9	78.1	74.8
	O 1s/O_β	33.9	67.6	60.8
Adsorption capacity (μmol/g)		83.3	82.1	76.1

The thermal stability of Mn-Si-MEL samples was detected and reflected in the Thermogravimetric-Differential Thermal Analysis (TG-DTA) curve (Fig. 1C). The main weight loss occurs in the temperature range of 300-550 °C, correlated to the combustion of the template that induces the formation of zeolitic framework. No additional weight loss was observed until 700 °C, demonstrating the superior stability of this zeolitic framework, which could be appli-

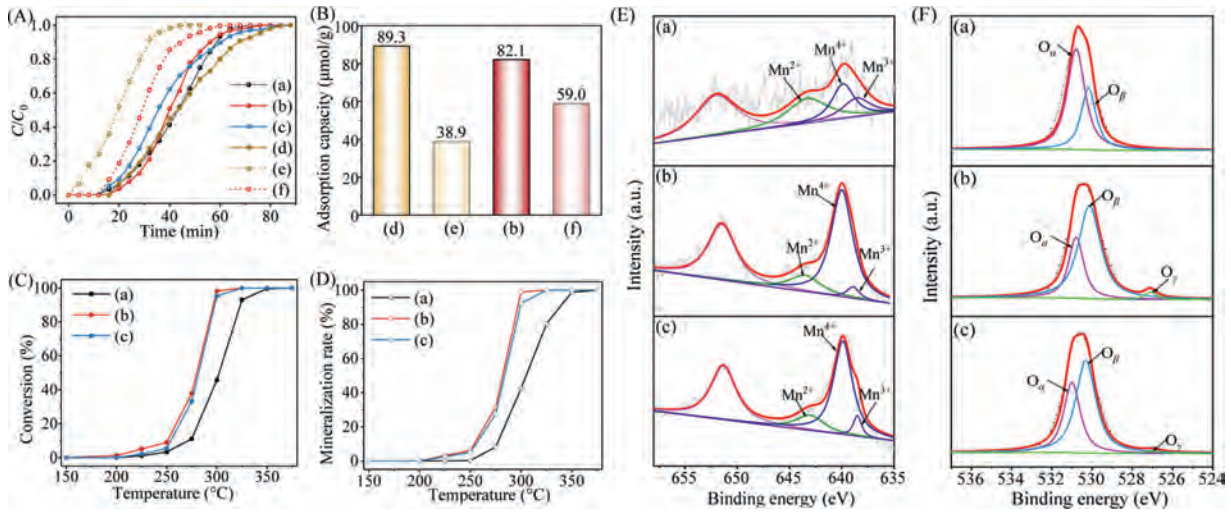

Fig. 2. Dynamic adsorption breakthrough curves (A), adsorption capacity (B), catalytic conversion curves (C), mineralization rate curves (D), Mn 2p X-Ray photoelectron spectroscopy (XPS) (E) and O 1s XPS (F) of various samples (a) Mn-S2(Seed), (b) Mn-S2(RC), (c) Mn-S2(DH), (d) Al-S2, (e) Al-S2-w (adsorption in presence of water vapor), (f) Mn-S2(RC)-w (adsorption in presence of water vapor).

cable in most industrial environments. Noting that two peaks in the DTA curve during the combustion of organic template present in both Mn-S2(RC) and Mn-S2(DH). As was analyzed in our previous work [15], the exothermic peak at higher temperature (~450 °C) is ascribed to the conventional combustion of organic template located in the channels of zeolite in presence of O_2, while the extra exothermic peak at lower temperature (394-404 °C) could be attributed to the fact that the formation of some reducible Mn species in the zeolite could act as a catalyst for promoting the combustion of organic template. Only a single peak was observed in Mn-S2(Seed) at higher temperature (446 °C), suggesting that the existence state of Mn species in zeolite *via* seeding method, by which Mn was impregnated in the seed crystals to be introduced into the initial gel, is much different from those by the other two methods. It seems that there is no reducible Mn species formed in Mn-S2(Seed). The Mn distribution in various samples was verified by the STEM-mapping images (Figs. 1B (a1-c2)). Mn-S2(Seed) has a uniform distribution of Mn species throughout the zeolite crystals (Figs. 1B (a1, a2)), while evident aggregation of Mn elements was found in both Mn-S2(RC) (Figs. 1B (b1, b2)) and Mn-S2(DH) (Figs. 1B (c1, c2)). Taking account of the TG-DTA analysis above, it is reasonable to believe these aggregated areas shown in the STEM images should be related to the Mn species with reducible ability. H_2-Temperature Programmed Reduction (H_2-TPR) (Fig. 1D) gave a verification about reducibility of various Mn-S2 samples again. Similar reduction profiles with two main reduction peaks, which were attributed to the reduction of Mn^{4+} to Mn^{3+} (low temperature) and Mn^{3+} to Mn^{2+} (high temperature) [21,22], were observed in all three samples, confirming the oxidation performance of these Mn-Si-MEL zeolites. Noteworthy is that Mn-S2(Seed) displays a shift to high temperature in both reduction peaks compared with the other two samples. This, on one side, implies the weaker reducibility of the former, on the other hand, confirms again the different Mn states & distribution of the former from the latter samples.

The bi-functional performance of Mn-Si-MEL zeolite as both a good adsorbent and a superior catalytic oxidation catalyst for VOCs elimination was tested by using toluene as a model pollutant molecular. As shown in Fig. 2A, the Mn-Si-MEL samples exhibit comparable dynamic adsorption behavior and capacity with the conventional Al-MEL (Al-S2) under dry gas, implying the good organophileproperty of Mn-Si framework similar to Si-Al framework. Nevertheless, in the presence of water vapor (11.5 mg/L), the Mn-Si-MEL sample (Mn-S2(RC)) displays much larger adsorption capacity (59.0 μmol/g) than that of Al-MEL (38.9 μmol/g) (Fig. 2B), suggesting the much better hydrophobicity of Mn-Si framework than the Si-Al framework. Fig. 1E gives a solid proof for the conclusion above. Different from the Al-S2 possessing the stretching vibration band of terminal Si-OH groups at ~3730 cm^{-1} [23], the band of less acidic hydroxyls at ~3650 cm^{-1} [24] and the bridging acidic hydroxyl stretching vibration at ~3590 cm^{-1}, all three Mn-S2 samples possess the main band at ~3730 cm^{-1} with no band at ~3650 cm^{-1} and very weak band at ~3590 cm^{-1}. As was reported from Prins *et al.* [25], although the groups mentioned above could all be able to adsorb polar compounds, the bridging Si-OH-Al groups are the most contributor to the strong binding with water. For Mn-Si-MEL samples, the absence of Al in the framework avoids the formation of hydrophilic structure and therefore, increases the zeolitic framework hydrophobicity. It should be mentioned that the bridging acidic hydroxyl is also a reflection of framework metal atoms [26,27]. The weak band at ~3590 cm^{-1} found in three Mn-S2 samples indicates that Mn could be involved in the formation of zeolitic framework of MEL by these methods, and the incorporation content of Mn into zeolite follows the sequence of Mn-S2(Seed) > Mn-S2(DH) > Mn-S2(RC), which is in good agreement with the STEM-mapping results mentioned above as well as the microporous properties priority of Mn-S2(Seed) > Mn-S2(DH) > Mn-S2(RC) listed in Table 1.

Superior catalytic activity is the other important key factor for evaluating the performance of bi-functional materials. Figs. 2C and D reflect the catalytic activity of toluene converted over three Mn-Si-MEL samples. Both Mn-S2(DH) and Mn-S2(RC) exhibit obviously superior catalytic activity for the deep oxidation of toluene compared with Mn-S2(Seed). Considering the reducibility of Mn species in three samples discussed above, it seems that the Mn species related to the zeolitic framework possess weaker oxidation than the extra-framework Mn species. X-Ray photoelectron spectroscopy (XPS) spectra of three Mn-Si-MEL samples were collected for verifying this deduction. As a surface analysis technique, XPS can well analyze the element state on the surface of catalysts. The weak signal of Mn-S2(Seed) once again confirms that the Mn is well incorporated into zeolite framework rather than distribute or aggregate on the surface of zeolite crystals like Mn-S2(DH) & Mn-S2(RC) (Fig. 2E). A spin-orbit doublet with Mn $2p_{3/2}$ (Bing energy (BE) of ~52 eV) and Mn $2p_{1/2}$ (BE of ~640 eV) appeared in all three Mn-S2 samples. According to peak-fitting deconvolutions,

three peaks Mn^{2+} (~643 eV), Mn^{3+} (~638 eV) and Mn^{4+} (~640 eV) were derived from Mn $2p_{3/2}$ [13]. The relative content of Mn^{4+} in total Mn species in Mn-S2(RC) & Mn-S2(DH) is much higher than that in Mn-S2(Seed) (Table 1), which might benefit from their higher extra-framework Mn species. A higher O_β (surface adsorbed oxygen species)/(O_α + O_β + O_γ) (total oxygen species = adsorbed oxygen from the hydroxyl species/adsorbed water species + surface adsorbed oxygen species + lattice oxygen) [28] ratio was also observed in both Mn-S2(RC) and Mn-S2(DH) compared with Mn-S2(Seed) (Fig. 2F and Table 1). It has been well reported that a high concentration of O_β and metal species with high oxidation state (Mn^{4+}) over a catalyst is beneficial for promoting the oxidation process [29]. Therefore, both the Mn-S2(RC) and Mn-S2(DH) exhibit much better higher oxidation ability for toluene than Mn-S2(Seed).

Based on these studies above, the Mn-S2(RC) with both satisfactory hydrophobic-adsorption capacity and catalytic oxidation performance for toluene was chosen for a cycling test. The adsorption capacity was well kept for Mn-S2(RC) after several cycles (Fig. S2 in Supporting information), demonstrating the potential application of this bifunctional Mn-Si-MEL zeolite in the enrichment-degradation of VOCs with low concentration. The life time test under humid condition was also performed for Mn-S2(RC) (Fig. S3 in Supporting information). The fact that the conversion of toluene could be kept at a high level in presence of H_2O also suggests its good potential to be applied in a humid atmosphere. Moreover, the GC-MS spectra (Fig. S4 in Supporting information) of toluene conversion over Mn-S2(RC) at different temperature was also taken for illustrating the conversion of toluene over Mn-Si-MEL, which follows from toluene firstly to intermediate organinc products (*i.e.*, benzaldehyde, phenol, octanal, diethylhexanol, phenylacetaldehyde, nonaldehyde, benzoic acid and decanal, *etc.*) and finally to CO_2 and H_2O for deep oxidation.

In summary, this work presents the potential of Mn-Si-MEL zeolite applied as a bi-functional adsorption-catalytic oxidation material for VOCs elimination. The substitution of Al by Mn in zeolite composition greatly improves the hydrophobicity of zeolites. Besides, the incorporation of Mn endows zeolites good catalytic oxidation despite their intrinsic adsorption properties. Three methods, including seeding method, recrystallization method and direct synthesis method were applied to introduce Mn into zeolite. It was found that the seeding method is favorable for the uniform distribution of Mn throughout zeolitic framework, while both recrystallization method and direct synthesis method are favorable for obtaining more reducible Mn species and surface adsorbed oxygen species, both of which benefit the catalytic combustion of toluene. Moreover, Mn-S2(RC) shows superior recyclability, confirming its potential to be a preferred candidate for the elimination of VOCs by an enrichment-degradation route.

Declaration of competing interest

The authors declare that they have no known competing financial interests or personal relationships that could have appeared to influence the work reported in this paper.

Acknowledgments

The authors greatly appreciated the finance supported by the Opening Fund of State Key Laboratory of Heavy Oil Processing (No. SKLOP202002001), the Program for Fundamental Research Funds for the Central Universities (No. FRF-AT-20-12), and National Natural Science Foundation of China (No. U20A20130).

Supplementary materials

Supplementary material associated with this article can be found, in the online version, at doi:10.1016/j.cclet.2021.09.072.

References

[1] Z. Chen, J. Li, X. Cheng, S. Zuo, Appl. Clay Sci. 163 (2018) 227–234.
[2] Z. Cheng, B. Feng, Z. Chen, et al., Chem. Eng. J. 392 (2020) 123747.
[3] H. Yamauchi, A. Kodama, T. Hirose, H. Okano, K.I. Yamada, Ind. Eng. Chem. Res. 46 (2007) 4316–4322.
[4] B. Chen, L. Wu, B. Wu, et al., ChemCatChem 11 (2019) 3646–3661.
[5] S.K.P. Veerapandian, N.D. Geyter, J.M. Giraudon, J.F. Lamonier, R. Morent, Catalysts 9 (2019) 98–137.
[6] S. Baek, J. Kim, S. Ihm, Stud. Surf. Sci. Catal. 154 (2004) 2458–2466.
[7] B.O. Adebayo, A. Krishnamurthy, A.A. Rownaghi, F. Rezaei, Ind. Eng. Chem. Res. 59 (2020) 13762–13772.
[8] Y. Wang, D. Yang, S. Li, et al., Microporous Mesoporous Mater. 258 (2017) 17–25.
[9] L. Zhang, Y. Peng, J. Zhang, et al., Chin. J. Catal. 37 (2016) 800–809.
[10] B. Yang, Y. Liu, M. Li, Chin. Chem. Lett. 27 (2016) 933–937.
[11] C. Chen, F. Chen, L. Zhang, et al., Chem. Commun. 51 (2015) 5936–5938.
[12] L. Wang, H. Zhang, Y. Yan, X. Zhang, RSC Adv. 5 (2015) 29482–29490.
[13] Y. Shu, M. He, J. Jia, et al., J. Hazard. Mater. 364 (2019) 770–779.
[14] T. Pang, X. Yang, C. Yuan, et al., Chin. Chem. Lett. 32 (2021) 328–338.
[15] H. Yi, Y. Feng, Q. Yu, et al., Sep. Purif. Technol. 251 (2020) 117363.
[16] Q. Yu, Y. Feng, X. Tang, et al., Microporous Mesoporous Mater 309 (2020) 110509.
[17] Q. Yu, X. Tang, H. Yi, Chem. Eng. J. 314 (2017) 212–222.
[18] Q. Yu, J. Chen, Q. Zhang, C. Li, Q. Cui, Mater. Lett. 120 (2014) 97–100.
[19] Q. Yu, C. Cui, Q. Zhang, et al., J. Energy Chem. 22 (2013) 761–768.
[20] Q. Yu, Q. Zhang, J. Liu, C. Li, Q. Cui, CrystEngComm 15 (2013) 7680–7687.
[21] C. Zhang, H. Huang, G. Li, et al., Catal. Today 327 (2018) 374–381.
[22] C. Zhang, C. Wang, W. Zhan, et al., Appl. Catal. B 129 (2013) 509–516.
[23] R. Joyner, M. Stockenhuber, J. Phys. Chem. B 103 (1999) 5963–5976.
[24] L. Meng, X. Zhu, B. Mezari, et al., ChemCatChem 9 (2017) 3942–3954.
[25] C.K.W. Meininghaus, R. Prins, Microporous Mesoporous Mater 35-36 (2000) 349–365.
[26] P. Lanzafame, G. Papanikolaou, S. Perathoner, et al., Appl. Catal. A 580 (2019) 186–196.
[27] I. Batonneau-gener, A. Yonli, S. Hazael-pascal, et al., Microporous Mesoporous Mater. 110 (2007) 480–487.
[28] M. Tian, M. Ma, B. Xu, et al., Catal. Sci. Technol. 8 (2018) 4503–4514.
[29] D. Meng, Q. Xu, Y. Jiao, et al., Appl. Catal. B 221 (2018) 652–663.